CIVED Journal of Civil Engineering and Vocational Education

EISSN: 2622-6774
Vol 12 No.1 March 2025
http://cived.ppj.unp.ac.id/index.php/CIVED

Structural Improvement Planning of Road Pavement with Modified Porous Asphalt Mixture using AASHTO 1993

Arief Aszharri[1*], Dimas Ariezky Susetyo[2], Nadra Mutiara Sari[3]
[1,2,3] Civil Engineering, Politeknik Negeri Sriwijaya, Indonesia
*Corresponding Author, e-mail: arief.aszharri@polsri.ac.id

Received 12th January 2025; Revision 21th January 2025; Accepted 15th February 2025

ABSTRACT

The new technology that is being developed is porous asphalt pavement structures, which are made for road segments with less dense traffic. This structure is designed to include facilities such as parking lots, bicycle lanes, pedestrian sidewalks, and tennis court areas. This study involves the analysis of calculation results based on secondary field data and experimental data from laboratory-scale experiments. The design of the road pavement is based on the AASHTO 1993 method. The field data used includes information on the LHR (Load History Record) of the Dawuan Highway (Cikampek) section, the CBR (California Bearing Ratio) value of the subgrade, and the existing pavement conditions (including existing pavement structures and deflection data). Meanwhile, experimental data comes from testing the resilient modulus of porous asphalt mixtures using Cariphalte asphalt and additional gilsonite material with optimal levels. The resilient modulus value was obtained from laboratory testing using the Universal Material Testing Apparatus (UMATTA). The results of this study produced a pavement design using a gilsonite mixture that produced a thinner thickness than standard AC-WC materials. For example, for segment 3 with a modified mixture, the pavement thickness is 13 cm, while the standard AC-WC produces a thickness of 20 cm. It can be seen that using a modified Gilsonite mixture requires an overlay layer 7 cm thinner than using a standard AC-WC mixture.

Keywords: *Porous Asphalt; Overlay; Thick Pavement Layer; AC-WC.*

DOI: https://doi.org/10.24036/cived.v12i1.688

INTRODUCTION

The new technology that is being developed is porous asphalt pavement structures, which are made for road segments with less heavy traffic. This structure is designed to include facilities such as parking lots, bicycle lanes, pedestrian sidewalks, and tennis court areas. In addition, this structure is also used as an alternative for water management or environmental conservation by considering water availability. This porous asphalt mixture acts as a surface layer in a flexible, environmentally friendly pavement structure, and is very suitable for vehicle parking areas. It is known as part of a pavement structure that allows water to seep [1]. According to recommendations from the U.S. Department of Transportation and the Federal Highway Administration (FHWA), a porous pavement structure should consist of three main layers: a surface layer, a filter layer, and a retention layer. All of these layers are built on soil that allows water to seep [2]. In several developed countries in America, Europe, and Asia, the use of porous asphalt mixtures has become a common practice that has long been developed and applied.

This has proven satisfactory results, especially in terms of water conservation. Countries such as Japan, the Netherlands, and several other countries have adopted porous asphalt mixtures as surface layers for flexible pavements with low traffic volumes, which also play a role in maintaining water availability [3]. Pavement structures using porous asphalt mixtures have a higher porosity level compared to conventional asphalt pavements. This high porosity is achieved by using more coarse aggregate in the porous asphalt mixture. However, this high porosity level can also affect the service life of the mixture due to its low stability [4]. Therefore, porous asphalt mixtures require the use of high-quality asphalt as an aggregate binder to maintain their stability. Therefore, further research is needed to determine how the structural performance of porous asphalt mixtures is reviewed from the thickness of the additional layer on a road section pavement with high traffic volume with LHR above 50,000 vehicles using cariphalte modified asphalt and the addition of gilsonite. This study will evaluate the pavement construction structure so that the thickness of the pavement structure layer will be obtained.

METHOD

Type of Research

This study involves the analysis of calculation results based on secondary field data and experimental data from laboratory-scale experiments. The design of the road pavement is based on the AASHTO 1993 method. The field data used includes information on the LHR (Load History Record) of the Dawuan Highway (Cikampek) section, the CBR (California Bearing Ratio) value of the subgrade, and the existing pavement conditions (including existing pavement structures and deflection data). Meanwhile, experimental data comes from testing the resilient modulus of porous asphalt mixtures using Cariphalte asphalt and additional gilsonite material with optimal levels. The resilient modulus value was obtained from laboratory testing using the Universal Material Testing Apparatus (UMATTA). Resilient modulus testing was carried out in various temperature ranges and loading frequencies to simulate environmental and traffic conditions in the field [5].

Structural Performance Analysis

Arimilli, et al (2017) stated that one of the techniques often used to plan pavement thickness is the AASHTO method [6]. This method has been widely adopted in various countries as a standard in road pavement planning. The AASHTO 1993 method is based on an empirical approach, which requires the following parameters:

a. Traffic Volume
b. Reliability Level
c. Environmental Influence
d. Desired Service (Serviceability)
e. Structural Number (SN)

The structural performance of a pavement can be expressed by determining the Structural Number (SN) or deflection value (DEF). The initial step in this analysis is to determine the SN value. SN is a pavement thickness index that is influenced by the thickness of each layer (Di), the relative strength coefficient of each layer (ai), and the drainage coefficient (mi). SN can be calculated using the AASTHO 1993 method using the formula in Equation (4.1). An illustration in the planning provisions using the AASTHO 1993 method is shown in Figure 1.

EISSN: 2622-6774
Vol 12 No.1 March 2025
http://cived.ppj.unp.ac.id/index.php/CIVED

SN = (a1 x D1) + (a2 x D2 x m2) + (a3 x D3 x m3)..(1)

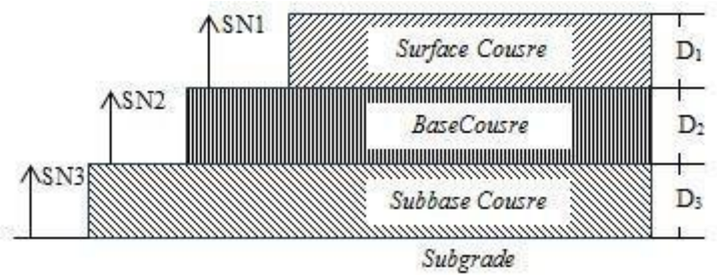

Figure 1. Determination of Structural Number AASTHO 1993 Method

In this discussion, the porous asphalt mixture will be used as the top layer of the road pavement structure, known as the surface course. The use of a porous asphalt layer aims to drain rainwater vertically and horizontally. The porous asphalt layer is planned to be placed on top of two other types of layers, namely the Asphalt Concrete Binder Course (AC-BC) and the Asphalt Concrete Wearing Course (AC-WC). Therefore, it is important that both types of layers, AC-BC and AC-WC, which are located under the porous asphalt layer, are in good condition and function as a waterproof layer [7]. This aims to prevent rainwater from seeping and flowing into the layers below the AC-BC and AC-WC, in accordance with the purpose of using porous asphalt that has been explained previously.

The structural performance analysis of the AC-WC surface layer was evaluated using secondary data obtained from the National Road Implementation Center (B2PJN) Region IV of West Java Province. The data includes:

1. Information on pavement conditions, including existing pavement structures and deflection data measured using a Falling Weight Deflectometer (FWD). Deflection measurements using FWD were carried out along the Dawuan (Cikampek) Highway section with a length of 4 km, with an average deflection measurement point every 400 meters.
2. The traffic volume data used is traffic data from 2016, which is the latest data currently available. Traffic growth calculations were carried out from 2016 to 2020, with the traffic growth rate calculated based on the average from 2016 to 2020.
3. The primary data used came from test results using the Universal Material Testing Apparatus (UMATTA) on porous asphalt mixtures in the laboratory, which provided a Resilient Modulus (MR) value. Information on the use of MR is used in calculating the relative coefficient value (a).

RESULTS AND DISCUSSION

Deflection Value Calculation

The deflection value was measured using FWD equipment in 2016. The initial stage in processing deflection data using the FWD tool was to segment the deflection in an effort to simplify the calculation and analysis process of the pavement structure.

Table 1. Deflection Value of Dawuan (Cikampek) Highway Section

No.	KM.	Tension (Kpa)	Load (kN)	Deflection (0,001 mm)									Temp. (^oC)		
				df1	df2	df3	df4	df5	df6	df7	df8	df9	$T_{pavement}$	$T_{surface}$	T_{air}
1.	0.000	581	41.05	149	181	141	103	78	56	41	29	26	39.6	44.2	31.8
2.	0.400	578	40.82	198	113	100	84	70	50	37	29	23	39.6	44.5	31.8
3.	0.800	567	40.10	155	121	106	90	76	54	39	30	25	39.6	41.3	31.8
4.	1.200	575	40.64	278	99	88	77	65	50	38	30	24	39.6	43.2	31.8
5.	1.600	569	40.24	247	275	212	158	124	83	65	56	48	39.6	44.1	31.8
6.	2.000	572	40.42	340	346	271	195	145	98	72	58	49	39.6	41.2	31.8
7.	2.400	573	40.50	388	152	134	114	97	70	53	41	35	39.6	40.8	31.8
8.	2.800	582	41.16	217	153	112	86	71	49	37	30	23	39.6	37.6	31.8
9.	3.200	569	40.21	349	269	201	145	109	72	51	40	34	39.6	39.5	31.8
10.	3.600	573	40.47	412	281	203	115	86	47	32	28	23	39.6	31.4	31.8
11.	4.000	572	40.45	222	130	117	101	88	62	45	35	28	39.6	41.0	31.8
Min		567	40.10	149	99	88	77	65	47	32	28	23	39.6	31.4	31.8
Max		582	41.16	412	346	271	195	145	98	72	58	49	39.6	44.5	31.8
Average		574	40.55	269	193	153	115	92	63	46	37	31	39.6	40.8	31.8

(Source: National Road Implementation Center Region IV, 2016)

Based on the representative deflection data from the load center point (D1) above, deflection segmentation is then carried out in an effort to simplify the calculation and analysis process of the pavement structure. Determination of deflection segmentation is also intended so that the calculation and analysis process of the overlay design is more effective. Because segmentation can simplify the deflection value of each FWD test point into several parts with an average deflection value that meets the uniformity factor requirements. Segmentation is carried out by trying to ensure that each segment has the same level of uniformity, namely <30% to avoid over design [8]. The deflection value used for the segmentation process is the deflection value at the load center (d1), this is because the deflection value d1 reflects the overall condition of the pavement layer from the surface layer to the base soil layer (Hossam, 2003). Based on Pd-T-05-2005-B that Uniformity Factor is divided into 3 groups, namely very good FK is a uniformity value of 0% - 10%, good FK is a uniformity value of 11% - 20% and quite good FK is a uniformity value of 21% - 30%. Thus, based on the calculation above, it is concluded that segment 1 has a good uniformity factor of 15.97% which is between the values 11% - 20%.

Table 2. Recapitulation of Deflection of Each Segment

Segmen	Load (kN)	Temp. (°C)	dR (0,001 mm)	dR(Inch)	S	Uniformity Factor (%)	Vice Deflection (Inch)	Vice Deflection (0,001 mm)
1	40.66	43.33	167	0.0659	0.0105	15.9723	0.087	220.787
2	40.33	42.87	227	0.0892	0.0252	28.2226	0.140	354.609
3	40.39	42.03	325	0.1280	0.0282	22.0574	0.184	468.374
4	40.62	39.30	318	0.1252	0.0352	28.1422	0.196	497.141
5	40.38	37.30	328	0.1290	0.0381	29.5364	0.205	521.282

Table 2 shows the representative deflection on the Dawuan Highway Section. The highest representative deflection is in segment five. With the different deflections between one segment and another, the structural strength of the pavement in each segment is also different. Likewise, the remaining service life and maintenance handling strategies are different.

Calculation of Effective Structural Number Value

SNeff is the capacity of the pavement structure during road testing using FWD in 2016. The effective Structural Number can be calculated on each segment obtained after segmentation to assess the performance of the pavement structure [9]. The calculation limit of the effective Structural Number used is the Kavussi et All method and the results of SNeffektif with this method can be seen in the table below. The results of the Kavussi et all equation for the strength of the existing pavement structure can be seen in Table 3.

Table 3. Calculation of SNeff Using the Kavussi et al Method

Segmen	Station	D0	D6	K1	K2	K3	SN_{eff}
1	0.000 - 0.800	167.333	53.300	34.171	-0.638	0.33	4.83985
2	0.800 - 1.600	226.667	62.367	34.171	-0.638	0.33	4.20005
3	1.600 - 2.400	325.000	83.733	34.171	-0.638	0.33	3.67818
4	2.400 - 3.200	318.100	63.833	34.171	-0.638	0.33	3.40948
5	3.200 - 4.000	327.700	60.333	34.171	-0.638	0.33	3.28373

The results of the SNeff calculation obtained using the Kavussi et all method show that each segment produces different values. This is due to differences in deflection data in each segment generated from FWD field data. The smallest SNeff value can be seen in segment 5, which is 3.283, which means that the pavement has the worst performance among the other segments. According to Hermasson, Åke. (2002), the selection of the Kavussi et all method provides calculation results similar to the calculation results using AASHTO which does not use assumptions outside of deflection data and the calculation results have a small standard deviation [10].

Traffic Calculation Plan

The traffic data used in this study is traffic data on the Dawuan Highway Section of West Java Province. Traffic volume and calculation of traffic growth rates in 2016 - 2021 can be seen in Table 4. The data used for the calculation stage of the Load Equivalency Factor (LEF) or often referred to as the equivalent number of axle loads on the vehicle axles are as follows. To calculate the load that occurs in the pavement structure, the ESAL factor grouping is carried out as seen in the table below. Design factors and axle load variations are calculated in 3 types of axles, namely the front, middle and rear axles.

Given:

a. Final surface index (Pt) = 2.5
b. Initial surface index (Po) = 4.2
c. Conversion of 1 ton (Lx) = 2.2046 Kips
d. Percentage of traffic growth (g) = 5%
e. Design life (n) = 5 years
f. L18 = 18 Kips
g. L2x = 1

Table 4. Results of Calculation of Total ESAL Factor (LEF)

No.	Vehicle Type	Description	Axis Config	Maximum Total Weight (Tons)	LEF			Total LEF (ESAL Factor)
					Front	Middle	Behind	
1	1	Motorcycles and Three Wheelers	-	-	-	-	-	-
2	2	Sedan, Jeep, St. Wagon	1.1	2	0.00026	-	0.00026	0.00052
3	3	Oplet, Pick-up & Minibus	1.1	2	0.00026	-	0.00026	0.00052
4	4	Pick Up, Micro Truck	1.1	5.3	0.00967	-	0.00967	0.01933
5	5a	Small Bus	1.2	9	0.01741	-	0.27732	0.29473
6	5b	Large Bus	1.2	14.2	0.11688	-	1.70191	1.81880
7	6a	2 Axle Truck (4 Wheels)	1.2	8.3	0.06194	-	0.06194	0.12387
8	6b	2 Axle Truck (6 Wheels)	1.2	18.2	0.15119	-	2.14724	2.29843
9	7a	3 Axle Truck	1.22	25	0.34197	-	1.58716	1.92913
10	7b	Towne Trailer	1.2+22	31.4	0.22538	1.33167	1.15909	2.71614
11	7c	Semi Trailer Truck	1.2-22	42	0.73829	3.98165	3.75330	8.47323
12	8	Non-Motorized Vehicles	-	-	-	-	-	-

Calculation of Resilient Modulus of Subgrade Soil

The segment subgrade resilient modulus (MR) is calculated using representative deflections at a certain distance according to the geophones used in the FWD tool. Determination of the MR value is carried out using the smallest geophone value, in this case using geophone number 9. Referring to AASHTO 1993, the subgrade resilient modulus value for planning is obtained by correcting the subgrade resilient modulus from the back deflection calculation with a correction factor of 0.33 (for FWD loads, ± 9000 lbs), to resemble the MR value in the pavement model from AASHTO Road Test Soil. Due to the segmentation of the road section being reviewed, the MR value obtained is also based on variations in the segmented deflection value [11].

Based on the FWD Tool test data to calculate the MR value, the data used are load data (p), deflection data (df) and distance data from the load center (r) from the 9th geophone which can be seen in Table 5. MR will be used in the AASHTO parameters which are calculated based on the segmentation division. After that, MR will be used to calculate the SN needed in the coming year.

Table 5. Segmentation Resilient Modulus

Station	P (kN)	P (Pound)	C	df9 (0,001 mm)	df9 (inch)	r9 (inch)	Mr (psi)
0.000 - 0.800	40.66	9140.03	0.33	25	0.00097	70.866	10547.08
0.800 - 1.600	40.33	9065.84	0.33	32	0.00126	70.866	8050.65
1.600 - 2.400	40.39	9079.33	0.33	44	0.00172	70.866	5906.84
2.400 - 3.200	40.62	9132.53	0.33	31	0.00121	70.866	8417.06
3.200 - 4.000	40.38	9077.08	0.33	28	0.00112	70.866	9062.30

Calculation of ESAL and CESA Using AASHTO 1993

After obtaining the MR value, LEF value and vehicle volume value, then proceed to the ESAL and CESA calculations to obtain the SNfuture value which is reviewed annually for five years of maintenance plan. ESAL is the planned traffic load obtained in that year while CESA is the cumulative load that will be reviewed in the future [12]. CESA is obtained by multiplying ESAL by Growth Factor (GF), lane distribution factor (DL), and direction distribution (DD). The Growth Factor (GF) value is used when the ESAL review is checked annually with a value (n) ranging from 1 to 5 because the maintenance age is reviewed for five years. While the DD value is taken as 0.45 while DL is a review of the number of lanes and directions.

Table 6. Design Traffic Calculation (ESAL)

Vehicle Type	Description	LHR 2019	LHR 2020	LHR 2021	2019 - 2020	
					Traffic ESAL Plan	Traffic Plan W18
1	Motorcycles and Three Wheelers	34586	36316	38131	-	-
2	Sedan, Jeep, St. Wagon	6833	7175	7534	7124	2885
3	Oplet, Pick-up & Minibus	984	1033	1085	1026	415
4	Pick Up, Micro Truck	2320	2436	2558	90463	36637
5a	Small Bus	171	180	189	101841	41246
5b	Large Bus	1474	1547	1625	5405744	2189326
6a	2 Axle Truck (4 Wheels)	4800	5039	5291	1199100	485636
6b	2 Axle Truck (6 Wheels)	0	0	0	0	0
7a	3 Axle Truck	2776	2915	3061	10800724	4374293
7b	Towne Trailer	247	259	272	1350748	547053
7c	Semi Trailer Truck	869	913	958	14857024	6017095
8	Non-Motorized Vehicles	75	79	83	-	-
Total W_{18}					13694586	

Direction distribution factor or DD can be seen in Pd. T-14-2003, but is generally taken as 0.45. While the lane distribution factor or DL is determined based on the number of lanes per direction so that the DL value is taken as 0.90 based on the number of lanes on the road section being reviewed is 2 per direction. Meanwhile, to evaluate the reviewed pavement structure, the W18 value per year is required.

$$W18 = D_D \times D_L \times W_{18}$$

$$= 0{,}50 \times 0{,}80 \times 14857024$$

$$= 13.694.586 \text{ ESAL}$$

Structural Number Future (SN_{future}) Calculation

SNfuture calculation can be done after getting ESAL or CESA value and MR data used as the result of segmentation division. To calculate SN_{future}, it is determined first by using certain parameters. The parameters used include reliability (R), overall standard deviation (SO), initial serviceability (PO), and terminal serviceability (Pt) [13]. For arterial roads, the R value used is 95% from the range of 85-99% so that the standard deviation (Z_R) value is obtained -1.645. The value is recommended for flexible pavement 0.45. The determination then determines the PO and Pt values with the respective values determined, namely 4.2 and 2.5. The results of the SN_{future} calculation can be seen in Table 9. After obtaining SN_{future} as the value of the results from predicting traffic loads in the design age, it is continued by calculating the handling of the pavement structure, namely the SCI (Structural Condition Index) value. The SCI value is taken from the result of dividing $SN_{effective}$ by SN_{future}. The results of the equation explain that the SCI value is smaller than 0.7 then the pavement structure requires an overlay, but if the SCI value is greater than 0.7 then the pavement structure does not require an overlay. The detailed SCI values can be seen in Table 7.

Journal of Civil Engineering and Vocational Education
EISSN: 2622-6774
Vol 12 No.1 March 2025
http://cived.ppj.unp.ac.id/index.php/CIVED

Table 7. Road Handling Based on SCI Value

SCI	Handling
>1	Routine Maintenance
0,7 – 1,0	Functional Overlay
0,5 – 0,7	Structural Overlay
< 0,5	Reconstruction

Treatment in the form of routine maintenance is carried out on the pavement structure in the form of crack covering or crack sealing, hole patching or potholing which does not provide additional reinforcement to the existing pavement structure but can reduce the rate of damage. While handling functional overlays can be in the form of thin re-coatings that do not provide an increase in the capacity of the pavement structure, if any, it is very small and ignored. Handling of structural overlays is a periodic maintenance activity by providing re-coatings that can provide additional capacity of the pavement structure in receiving repetitive loads for the future. Determination of overlay thickness is calculated based on the current capacity value and future capacity according to the planned service period [14]. Therefore, the following discussion will only discuss segments that require structural overlays. The results of the evaluation of handling based on SCI criteria are shown in Table 8 and Table 9.

Table 8. Pavement Structure Handling During 2019 – 2021

Segmen	Station	$SN_{effektif}$	2019		2020		2021	
			SCI	Keterangan	SCI	Keterangan	SCI	Keterangan
1	0.000 - 0.800	4.839852	1.092871	Routine Maintenance	0.984532	Functional Overlay	0.927443	Functional Overlay
2	0.800 - 1.600	4.200052	0.894934	Functional Overlay	0.808408	Functional Overlay	0.762632	Functional Overlay
3	1.600 - 2.400	3.678177	0.74348	Functional Overlay	0.673366	*Structural Overlay*	0.636	*Structural Overlay*
4	2.400 - 3.200	3.409477	0.799756	Functional Overlay	0.719181	Functional Overlay	0.676802	*Structural Overlay*
5	3.200 - 4.000	3.283731	0.723967	Functional Overlay	0.65293	*Structural Overlay*	0.615443	*Structural Overlay*

Table 9. Thickness of Modified, Normal and Standard Porous Asphalt Overlay Layers

Year	Segmen	$SN_{effektif}$	SN_{future}	$SN_{overlay}$	Modification		Normal		Standard	
					a	$D_{overlay}$ (cm)	a	$D_{overlay}$ (cm)	a	$D_{overlay}$ (cm)
2021	3	3.284	5.562	2.278	0.404	14	0.403	13	0.27	20
2021	4	3.409	5.038	1.628		10		10		16
2021	5	3.284	5.336	2.052		13		13		20

Structural Overlay Design

The design of structural overlay handling on an existing pavement structure on the Dawuan Highway Section is based on Table 9 according to SCI parameters. Thus, the implementation of additional layers or overlays only occurs in 2021 carried out on segments 3, 4 and 5. Continued by calculating the overlay thickness requirements resulting from the difference in the results of the planned structural capacity requirements in the future (SN_{future}) with the effective structural capacity and divided by the relative coefficient (a) from the UMATTA test results to obtain the modulus of elasticity of the overlay layer [15]. After that, it is continued with the modulus of elasticity value of the overlay layer from MDP 2017 to obtain the value of a as a comparison of the test results that have been carried out. The results of the overlay thickness calculation can be seen in Table 9. Table 9 shows the thickness of each periodic maintenance or overlay by comparing the materials used, namely modified, normal and standard porous asphalt planning. The thickness obtained by the modified and normal porous asphalt mixtures gives the same results. Previously, the modulus of elasticity value was used to find the value of a1 using the equation below. The E value is the same as the elastic modulus value in MPa units or can be seen in Table 10. The results of the modified elastic modulus value are obtained from the results of the characteristics of the optimum 7% porous asphalt mixture. The normal mixture uses 0% gilsonite and the standard AC-WC mixture elastic modulus refers to the 2017 MDP, which is 1,100 MPa.

Table 10. Coefficient Values for Each Porous Asphalt Pavement Model

Mixed Type	**MR (Mpa)**	**a**
Modification	2.444	0,404
Normal	2.422	0,403
Standard	1.100	0,266

After obtaining the SN_{future} and SN_{eff} values in Table 9, it is continued by calculating $SN_{Overlay}$. Then the pavement thickness calculation is carried out using the a1 value which can be seen in Table 10 from each type of mixture.

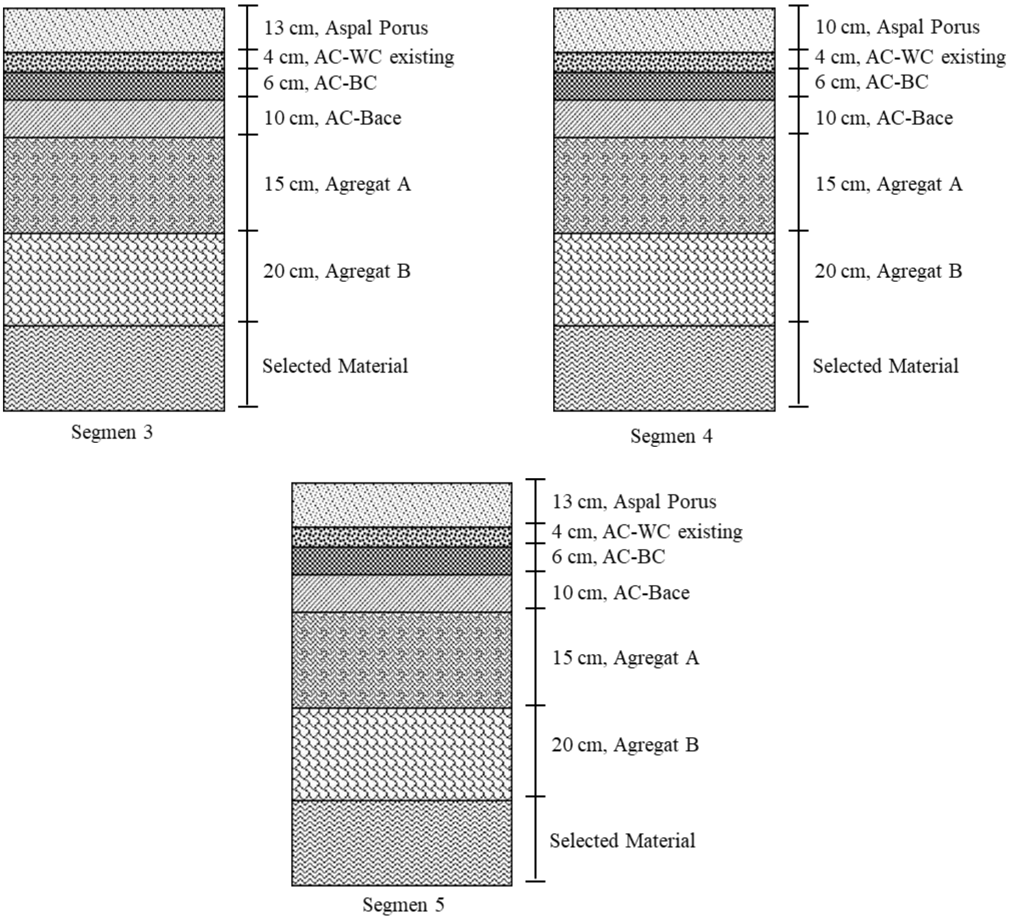

Figure 3. Design of Modified Porous Asphalt Mix Overlay with Gilsonite and Normal Mix in Segments 3, 4, and 5

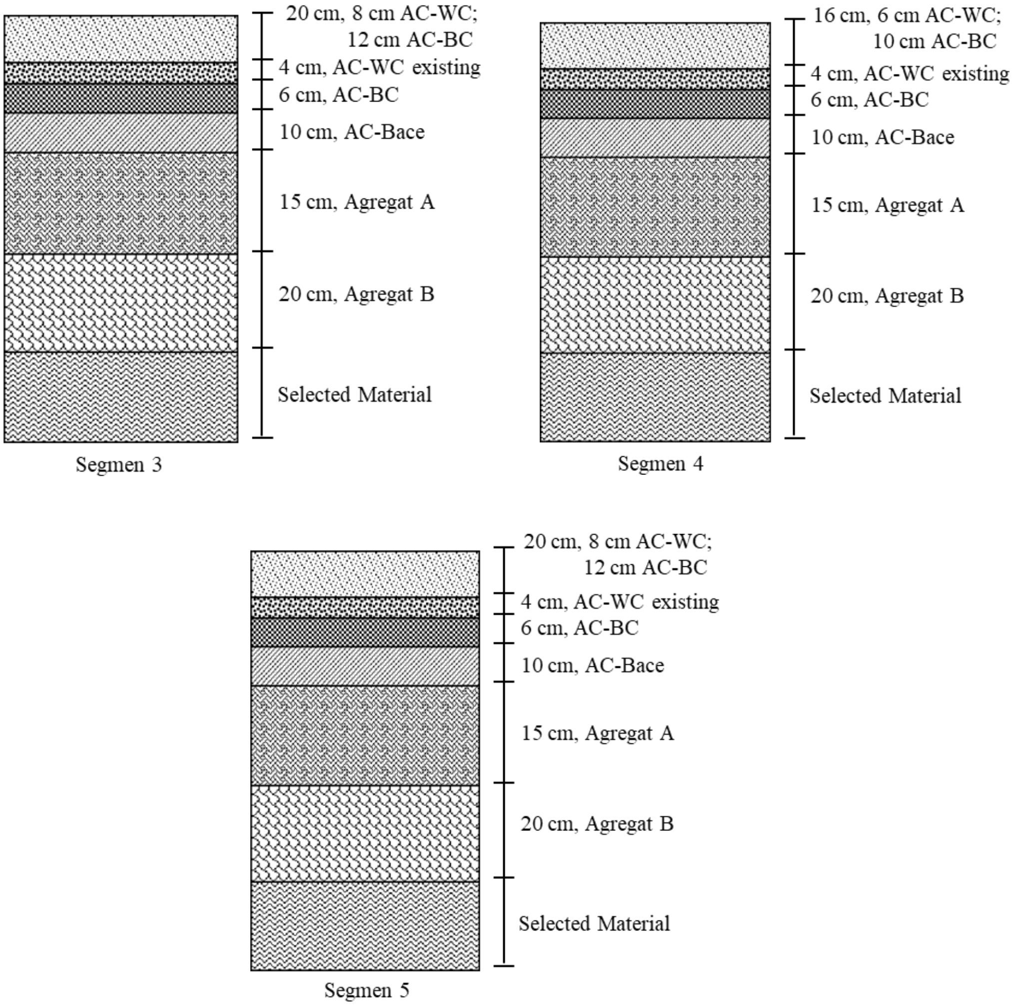

Figure 4. Standard AC-WC Mixed Overlay Design on Segments 3, 4, and 5

Based on Figure 3 and Figure 4 above, it can be seen that the pavement design using a gilsonite mixture produces a thinner thickness than the standard AC-WC material. For example, for segment 3 with a modified mixture, the pavement thickness is 13 cm, while the standard AC-WC produces a thickness of 20 cm. It can be seen that using a modified gilsonite mixture requires an overlay layer that is 7 cm thinner than using the standard AC-WC mixture. Figure 4 is a model of the pavement structure using a standard AC-WC mixture where the thickness used must be divided into two parts, namely the AC-WC thickness and the AC-BC thickness.

This is done so that the pavement structure remains strong and also economical. In the AC-BC pavement structure, a thickness of 12 cm is planned and the rest is the AC-WC surface, namely in segments 3 and 5 the AC-WC pavement structure has a thickness of 8 cm while segment 4 has 6 cm. In addition to porous asphalt can be used as a surface layer on a flexible pavement structure, the porous asphalt layer can also be used as part of a porous asphalt pavement structure where one of the layers functions as a reservoir/stone recharge bed. From the secondary data obtained, on the Dawuan Highway section, it can be planned to widen the road by 1.5 m for the left side and 1.5 m for the right side of the road. Furthermore, the road widening will use a porous asphalt pavement structure where one of the layers functions as a reservoir so that rainwater flowing vertically and horizontally from the porous asphalt layer will be channeled to the choker course then to the stone recharge bed and then continued to the drainage. Thus, rainwater is not entirely forwarded to the road drainage. Some of the water will be stored in the stone recharge bed which will be installed underneath Woven geotextile.

The use of this type of geotextile is because it is waterproof so that water does not flow into the ground so that there is no damage to the base soil. The water stored in the stone recharge bed is as a water reserve in case of a dry season [16]. Choker course consists of clean single-size crushed stone that is smaller than the stone in the stone recharge bed. Choker course functions to stabilize the surface structure of the pavement by filling several surface cavities and locking the aggregate. The thickness of each layer will be calculated based on the previously obtained SNfuture value. The relative strength coefficient of Choker Coarse (a2) and the relative strength coefficient of Stone Recharge Bed (a3) used are Choker Coarse 0.30-0.35 and Stone Recharge Bed 0.10-0.14 (Hansen, 2008). The porous asphalt pavement structure on road widening using porous asphalt as the surface layer functions as a reservoir as seen in Figure 5.

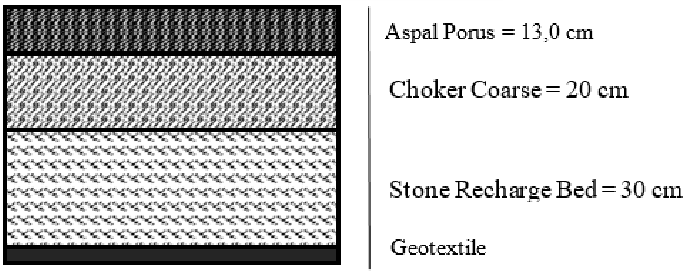

Figure 5. Porous Asphalt Pavement Structure for Road Widening

CONCLUSION

Based on the results of the analysis conducted, it can be concluded as follows:
1. The productivity value of crawler cranes is, in reality, direct observation has a higher productivity value of 1.51 units/hour compared with theoretical calculations, which only get a value of 1.060 units/hour.
2. In the theoretical calculation, it is said that the girder erection work is carried out in a total cycle time of 15.1 hours. It can be concluded that the girder erection work is estimated to be carried out for 2 days, with the duration of effective hours per day being 8 hours. Meanwhile, in direct observation, it is known that the total cycle time required is only 10.58 hours in the calculation. From these results, it can be concluded that the girder erection work can also be done within 2 days. However, in reality, the girder erection work was carried out for 5 days.
3. The main factor causing delays in girder erection work is weather conditions at the time, causing the girder erection process to be canceled and postponed. In addition, several factors also affected the delay of girder erection work at that time, such as operational constraints and the operators' efficiency.

REFERENCE

[1] J. N’Cho, "Contribution of talent analytics in change management within project management organizations The case of the French aerospace sector," *Procedia computer science*, vol. 121, pp. 625-629, 2017, doi: https://doi.org/10.1016/j.procs.2017.11.082.
[2] A. Nursin, F. Fitria, and T. W. Sari, "Last Planner System pada Proyek Rumah Susun

EISSN: 2622-6774
Vol 12 No.1 March 2025
http://cived.ppj.unp.ac.id/index.php/CIVED

Transit Oriented Development," in *Prosiding Seminar Nasional Teknik Sipil*, 2020, pp. 32-40. [Online]. Available:https://prosiding-old.pnj.ac.id/index.php/snts/article/download/3612/2038?__cf_chl_tk=YwJ8VDZUmMYEOGDySnLtQSk7btcYqadsrShaUVxaBi0-1735009117-1.0.1.1-8af8ylPgvvfTfFKwZxB.QjeS7OAFapkT0PEUsbg7F_0.

[3] B. B. Kalengkongan, T. T. Arsjad, and J. B. Mangare, "Analisa Perhitungan Produktivitas Alat Berat Pada Pekerjaan Pematangan Lahan Pembangunan Tower Sutet Likupang-Paniki," *Jurnal Sipil Statik*, vol. 8, no. 1, 2020. [Online]. Available: https://ejournal.unsrat.ac.id/index.php/jss/article/view/27722/0.

[4] A. Setiobudi, "Pengujian Kuat Tekan Beton Mutu Tinggi Type Fcâ€™ 50 (Kelas Aa) Untuk Girder Jembatan Di Tol Palembang Indralaya (Palindra)," *Jurnal Deformasi*, vol. 2, no. 1, pp. 7-25, 2017, doi: https://doi.org/10.31851/deformasi.v2i1.1200.

[5] D. Wijanarko and R. W. Rahmadi, "Optimalisasi Produksi Alat Berat Dalam Pekerjaan Galian Dan Tanaman Di Proyek Jalan Raya (Studi Kasus: Jalur Lintas Selatan Lot 2 Blitar)," *Jurnal Daktilitas*, vol. 4, no. 01, pp. 25-36, 2024. [Online]. Available: https://journal.unita.ac.id/index.php/daktilitas/article/view/1157/669.

[6] S. S. Chandra, S. M. Sepasgozar, V. R. P. Kumar, A. K. Singh, L. Krishnaraj, and B. O. Awuzie, "Assessing factors affecting construction equipment productivity using structural equation modeling," *Buildings*, vol. 13, no. 2, p. 502, 2023, doi: https://doi.org/10.3390/buildings13020502.

[7] A. Maddeppungeng, S. Asyiah, D. E. Intari, B. I. Hakim, and D. N. Setiawati, "Analysis of Heavy Equipment Productivity Tower Crane in The Construction Project of Sultan Maulana Hasanudin State Islamic University Building," *Fondasi : Jurnal Teknik Sipil*, vol. 12, 2023, doi: https://dx.doi.org/10.36055/fondasi.v12i2.21982.

[8] D. Hadiyatmoko, J. U. D. Hatmoko, and M. A. Wibowo, "Analysis of Launcher's Productivity in Erection Girder Using Time Motion Study Method," *Civil Engineering Journal*, vol. 9, no. 8, pp. 1897-1911, 2023, doi: http://dx.doi.org/10.28991/CEJ-2023-09-08-06.

[9] I. A. Ahmad and M. S. HS, "Analisis Produktivitas Dan Biaya Operasional Tower Crane Pada Proyek Puncak Central Business District Surabaya," *Jurnal Rekayasa Teknik Sipil*, vol. 2, no. 2, pp. 1-12, 2018. [Online]. Available: https://core.ac.uk/outputs/230737552/?utm_source=pdf&utm_medium=banner&utm_campaign=pdf-decoration-v1.

[10] G. w. Subagyo and R. Tjondro, "Analisis Produktivitas Tower Crane (Studi Kasus Proyek Bintaro Jaya Xchange Tahap II, Tangerang Selatan)," *Indonesian Journal Of Construction Engineering And Sustainable Development (CESD)*, vol. 4, 2021, doi: https://doi.org/10.25105/cesd.v4i2.12510.

[11] E. Hasdian, M. A. Maulana, N. C. Fertilia, and Y. Lutfiansyah, "Analysis Comparissons of Ereciton Girder Implementations Methods Using Laucher Gantry and Crawler Crane Based on Cost and Time:(Case Study: Cimanggis-Cibitung Toll Road Project Section II Cibubur Area)," *ADRI International Journal of Sciences, Engineering and Technology*, vol. 6, no. 2, pp. 78-88, 2021. [Online]. Available: http://adri.journal.or.id/index.php/ijset/index.

[12] A. Salsabila, R. T. Iriana, S. Djuniati, M. Sebayang, and E. Elianora, "Optimalisasi Penempatan Tower Crane Pada Proyek Pembangunan Gedung Pascasarjana, Universitas Riau," *Jurnal Ilmiah Rekayasa Sipil*, vol. 21, no. 2, pp. 253-265, 2024, doi: https://doi.org/10.30630/jirs.v21i2.1425.

[13] S. M. Hastanto and F. Ratu Gudam, "Studi Kasus Perubahan Letak Dan Pondasi Tower Crane Static Menjadi Tower Crane Climbing Pada Proyek at District 8 Senopati Jakarta

Selatan," *Jurnal Forum Mekanika*, vol. 5, no. 1, pp. 53-60, 2016 2016, doi: 10.33322/forummekanika.v5i1.641.

[14] V. Mergl and J. Kašpárek, "Verifying the lifting and slewing dynamics of a harvester crane with possible levelling when operating on sloping grounds," *Forests*, vol. 13, no. 2, p. 357, 2022, doi: https://doi.org/10.3390/f13020357.

[15] A. R. Umar and P. R. T. Naibaho, "Analisa Perbandingan Pelaksanaan Erection Girder Underpass pada Jalan Nasional dengan Metode Crane dan Metode Launcher," *Asian Journal of Mechatronics and Electrical Engineering*, vol. 1, no. 1, pp. 1-12, 2022, doi: https://doi.org/10.55927/ajmee.v1i1.1122.

[16] E. N. Kulo, J. E. Waani, and O. H. Kaseke, "Analisa Produktivitas Alat Berat Untuk Pekerjaan Pembangunan Jalan (Studi Kasus: Proyek Pembangunan Jalan Lingkar SKPD Tahap 2 Lokasi Kecamatan Tutuyan Kabupaten Bolaang Mongondow Timur)," *Jurnal Sipil Statik*, vol. 1, no. 7, 2017, doi: Prefix 10.55927.

[17] M. Indrayadi and R. Pratiwi, "Analisa Produktivitas Peralatan Konstruksi Pada Proyek Pembangunan Infrastruktur Universitas Tanjungpura (IDB)," *JeLAST: Jurnal Teknik Kelautan, PWK, Sipil, dan Tambang*, vol. 5, no. 3, doi: https://doi.org/10.26418/jelast.v5i3.30317.